Sensing With Slow Light in Fiber Bragg Gratings

He Wen, Matt Terrel, Shanhui Fan, *Fellow, IEEE*, and Michel Digonnet, *Member, IEEE*

***Abstract*—On the edge of the bandgap in a fiber Bragg grating (FBG) narrow peaks of high transmission exist at frequencies where light interferes constructively in the forward direction. In the vicinity of these transmission peaks, light reflects back and forth numerous times across the periodic structure and experiences a large group delay. Since the sensitivity of a phase sensor to most external perturbations is proportional to the reciprocal of group velocity, in these slow-light regions the sensitivity of an FBG is expected to be significantly enhanced over traditional FBG sensors operated around the Bragg wavelength. In this paper, we describe means of producing and operating FBGs that support structural slow light with a group index that can be in principle as high as several thousand. We present simulations elucidating how to select the FBG parameters, in particular index modulation, length, and apodization, to generate such low group velocities, and quantify the very large improvement in strain and temperature sensitivities resulting from these new slow-light configurations. As a proof of concept, we report an FBG with a group index of 127, or a group velocity of $\sim 2{,}360\ \mathrm{km/s}$. This is by far the lowest group velocity reported to date in an FBG. Used as a strain sensor, this slow-light FBG is shown to be able to detect a strain as small as 880 $\mathrm{f}\varepsilon/\sqrt{\mathrm{Hz}}$, the lowest value reported for a passive FBG sensor.**

***Index Terms*—Bragg gratings, fiber gratings, optical fiber sensors, slow light.**

I. Introduction

FIBER Bragg gratings (FBGs) are used extensively in research and in industry for many photonics applications, in particular, in communication systems, in fiber lasers, and in fiber sensors. In the field of fiber sensors, they are widely used to sense a number of perturbations, especially strain and temperature. When a strain change is applied to an FBG, three of the FBG parameters change, namely, its length L (through stress on the fiber) and therefore the grating period Λ, the material index, and the mode effective index (through the change in the fiber core dimensions). These three changes result in a shift in the Bragg wavelength λ_B. This shift can be detected with an optical spectrum analyzer (OSA), but the sensitivity is limited by the resolution of the OSA, which is typically 0.05 nm. It can also be detected using a Mach–Zehnder interferometer (MZI) to convert the wavelength shift to an amplitude shift. The sensitivity is then proportional to the path difference between the two arms of interferometer. However, this path difference can only be increased so much, as discussed further on. In spite of this limitation, we believe this MZI scheme holds the record for the lowest minimum detectable dynamic strain in a passive, non-slow-light FBG sensor (600 $\mathrm{p}\varepsilon/\sqrt{\mathrm{Hz}}$) [17].

In this work, we report a novel sensing scheme that uses structural slow light in an FBG and improves this resolution record substantially. The basic premise is that the phase shift induced by a perturbation applied to a device, for example, a fiber or an FBG, is proportional to the reciprocal of the group velocity v_g [1]. When the group velocity is reduced, this phase shift is therefore increased [2]. The ability to generate slow light in a fiber, therefore, offers the compelling prospect of a new generation of sensors with greatly enhanced sensitivity over conventional FBG-based sensors.

Three physical mechanisms have been investigated to date to obtain slow light in a fiber, namely, electromagnetically induced transparency (EIT) [3], stimulated Brillouin scattering (SBS) [4], and fiber Bragg gratings (FBGs) [5]. EIT is the most promising method for generating extremely slow light [3], but it is currently impeded by undesirable reaction between Rb and the silica host. SBS is more practical, but it produces modest velocity reductions limited by the SBS gain. For example, in an SBS fiber amplifier a group velocity of $v_g = 71{,}000\ \mathrm{km/s}$ (or a group index $n_g \approx 4.2$) has been demonstrated [4]. A group velocity of 30 000 km/s ($n_g = 10$) was reported using SBS in a 2-m bismuth-oxide optical fiber [6]. Both EIT and SBS require supplying power to the fiber, and long lengths of fiber in the case of SBS.

In contrast, an FBG offers a much simpler and more practical alternative because it relies on a passive resonant effect and thus does not need an optical pump. It is also a very short and inexpensive component. As we will see, an FBG can produce large group-velocity reductions and reasonable group delays, although unfortunately the latter are not tunable. Applications requiring large group indices, such as sensing, will therefore greatly benefit from using slow light in an FBG. The presence of a periodic structure in an FBG induces a band of finite bandwidth in the frequency space, where light is not allowed to propagate. Stated differently, when light in the vicinity of λ_B is injected into an FBG, it is substantially reflected, while light sufficiently detuned from λ_B is transmitted. It is well-known that on the edges of a photonic bandgap there are frequencies where the group velocity is decreased. This is true also of an FBG, which is a one-dimensional photonic crystal. A simple analogy is a Fabry–Perot interferometer, in which at well-defined evenly spaced frequencies light travels back and forth between two reflectors and experiences a decrease in net group velocity. In an FBG, the situation is analogous, except that because of the distributed nature of the reflector (a periodic structure) the reflectivity is a strong function of frequency and of the structure period. These differences result, as we will see, in a completely different, non-periodic slow-light spectrum.

Manuscript received November 16, 2010; revised February 17, 2011; accepted March 09, 2011. Date of publication April 05, 2011; date of current version December 01, 2011. This work was supported in part by Litton Systems, Inc., a wholly owned subsidiary of Northrop Grumman Corporation. The associate editor coordinating the review of this paper and approving it for publication was Prof. Jose Lopez-Higuera.

The authors are with the Center for Nanoscale Science and Technology, Stanford University, Stanford, CA 94305 USA (e-mail: vickywen@stanford.edu; terrel@stanford.edu; shanhui@stanford.edu; silurian@stanford.edu).

Digital Object Identifier 10.1109/JSEN.2011.2135343

1530-437X/$26.00 © 2011 IEEE

Surprisingly, investigations of slow light in FBGs have been very limited. Simulations showed that in a uniform FBG, the group index is maximum in the vicinity of the first transmission peak on either side of the Bragg-wavelength reflection peak [7]. For an FBG with a length of 2.67 cm and an index contrast $\Delta n = 10^{-4}$, a group index of 3.3 was predicted around 1550 nm. This effect had been used previously in a 10-cm apodized silica FBG with a Δn of 1.53×10^{-4} to produce solitons with a group index of ~ 5 [5]. Gap solitons with a pulse delay equal to 20 times the pulse width have also been predicted through simulations in a 10-cm FBG with a Δn of 10^{-3} [8], which corresponds to an inferred group index of ~ 39.

The purpose of this work was threefold. First, we wanted to develop a model that predicts how much further the group velocity of light can be reduced in an FBG, and how to design an FBG for slowest light. Second, we wanted to verify experimentally the predictions of this model and demonstrate by the same token a much slower group velocity than ever before. Finally, we wanted to demonstrate a slow-light FBG strain sensor with a much higher sensitivity than comparable FBG strain sensors.

Our modeling efforts show that to maximize the group index attainable at certain band-edge frequencies in an FBG, the index modulation should be as large as possible, and the loss as low as possible. For a given loss, there is also a grating length that maximizes the group index. In addition, apodization can significantly increase the group index. Based on these findings, it appears that a main reason why slower light has not been observed in the past in FBGs is that most FBGs have either a weak index modulation, or that their length was too short or not optimized. Using a commercial FBG with suitable apodization and a large index modulation of $\sim 10^{-3}$, we measured a group index as large as 127, the highest value reported in FBG to date. The same FBG used in a new, slow-light dynamic strain sensing scheme gave a sensitivity of 3.14×10^5 strain^{-1} and a minimum detectable strain (MDS) of 880 f$\varepsilon/\sqrt{\text{Hz}}$. To the best of our knowledge, this is ~ 6 times lower than the previous minimum detectable strain record reported in a passive FBG strain sensor [19].

II. Theory

A. Modeling Slow-Light in an FBG

Coupled-mode theory was used to calculate the complex amplitude spectrum of the signal transmitted by the FBG (see, e.g., [9]). The real part of the transmitted amplitude spectrum provided the power spectrum of the signal transmitted by the FBG; the imaginary part provided the transmitted phase spectrum. The group index spectrum $n_g(\omega)$ for the transmitted signal was then calculated as the derivative of the phase spectrum $\theta_t(\omega)$ using

$$n_g = \frac{c\tau_t}{L} = \frac{c}{L}\frac{d\theta_t}{d\omega}. \tag{1}$$

In the special case of a uniform grating (constant Δn), the coupled-mode equations have an analytical solution for the fields [10]. For nonuniform gratings, such as apodized, chirped, π-shifted, they can be solved by either numerical integration or a piecewise uniform approach. The approach we followed is the latter. It consists in dividing the grating into many sections short enough that the index modulation in each section can be assumed uniform [9]. Our analysis focused on the impact on the group index spectrum of the index profile (uniform or apodized), index modulation Δn, grating length L, and power loss coefficient α of the FBG , with a view towards tailoring these parameters to minimize the group velocity.

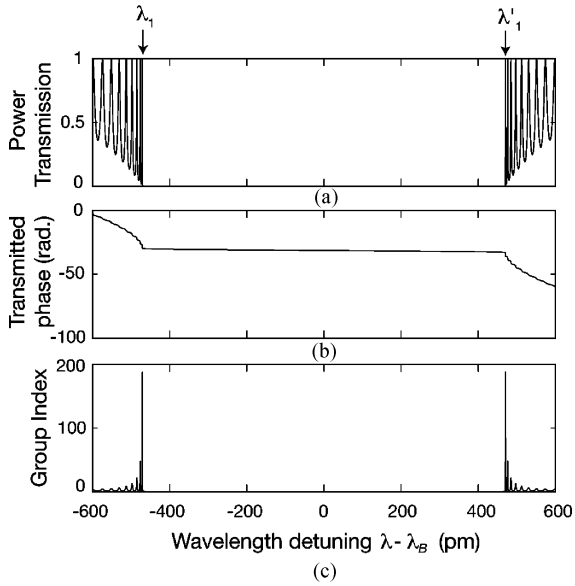

Fig. 1. Simulated transmission, phase, and group index spectra of a lossless uniform FBG.

Fig. 1(a) and (b) show the calculated power and phase spectra of the signal transmitted by a lossless uniform silica-fiber Bragg grating with a period $\Lambda = 0.534\,\mu$m (Bragg wavelength $\lambda_B = 1.55\,\mu$m), $\Delta n = 1.0 \times 10^{-3}$, and $L = 2$ cm. This grating is much stronger than a standard communication grating ($\Delta n \approx 10^{-6} - 10^{-4}$). As a result, its transmission exhibits sizable side-lobes on either side of its Bragg reflection peak. The phase varies comparatively slowly at all frequencies, except in the vicinity of the side-lobes, where slow light exists. The magnitude of this effect can be better seen in Fig. 1(c), which plots the group index spectrum, calculated from the derivative of the phase spectrum using (1). In the vicinity of the wavelengths λ_1 and λ_1' where the transmission approaches unity [see Fig. 1(a)], the group index peaks at ~ 187, which is significantly larger than the group index of ~ 1.44 that prevails for large detunings from λ_B. Because light is slowest in the vicinity of transmission maxima, an FBG can be used in these slow-light bands with little power attenuation.

Simulations show that for a fixed length ($L = 2$ cm), the group index increases rapidly with Δn, approximately as $\Delta n^{1.99}$ [see Fig. 2(a)]. For a fixed index contrast $\Delta n = 10^{-3}$, the group index increases approximately as $L^{1.9}$ [see Fig. 2(b)]. These superlinear dependences show that a tremendous increase in group index can be achieved even with modest increase in length and/or index contrast. For example, a 10-cm lossless uniform grating with an index contrast of 1.5×10^{-2} (which is readily attainable in a hydrogen-loaded fiber) [11] is predicted to support light with an n_g as large as $\sim 10^6$, or a group velocity of only ~ 300 m/s. The conclusion is that significantly slower light can be induced in an FBG provided the index modulation and/or the length are increased substantially beyond the ranges of values probed until now.

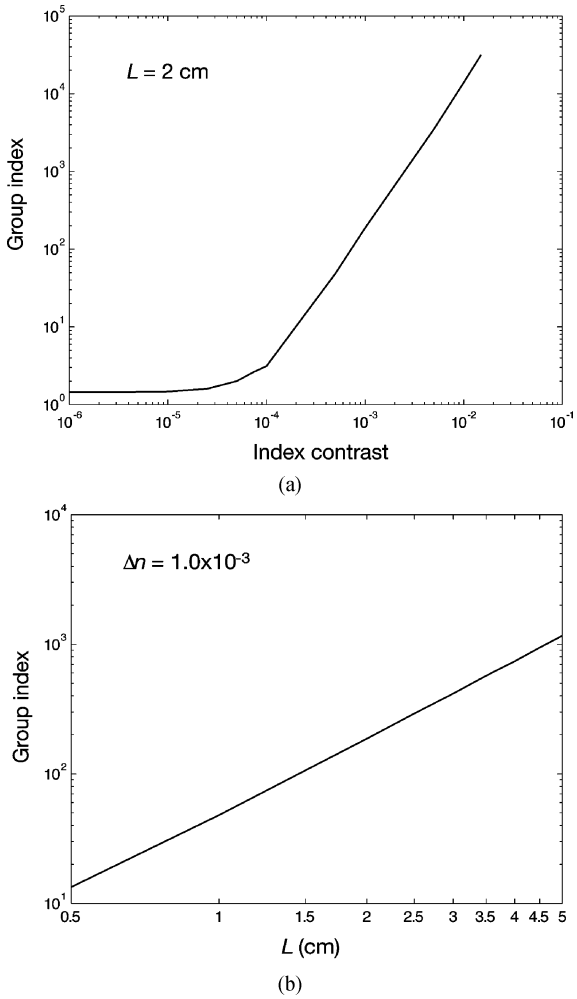

Fig. 2. Calculated dependence of the group index of a lossless uniform FBG on: (a) index contrast and (b) length.

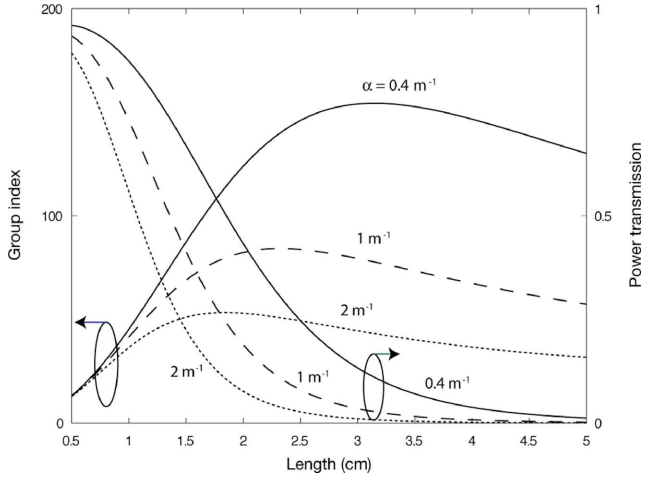

Fig. 3. The dependence of group index and transmission on length for gratings with different loss coefficients.

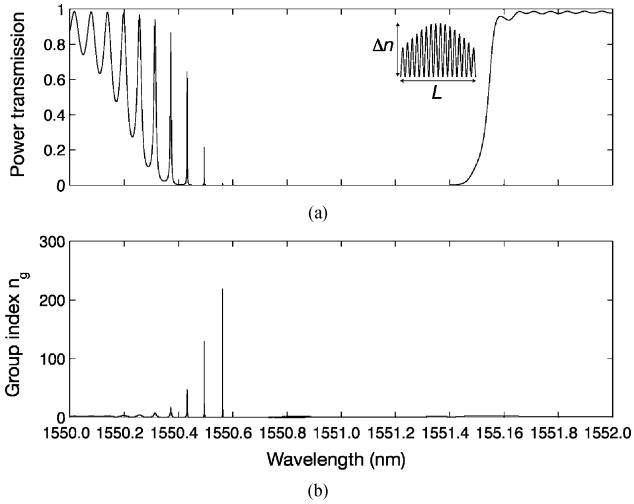

Fig. 4. Calculated (a) transmission and (b) group index spectrum of an apodized FBG.

In practice, loss does not only reduce the transmission of an FBG; it also limits the maximum achievable group index. Reported power loss coefficients range from greater than 5.8 m^{-1} for an H_2-loaded grating [13] to 1 m^{-1} for a conventional UV-written Ge-doped silica FBG [12] and less than 0.4 m^{-1} for strong FBG fabricated with ultrashort pulses in Corning's SMF-28 fiber [14]. These values depend on a number of parameters, including the index modulation. Because of this loss, the group index no longer increases indefinitely with length, but there is an optimum length for which the group index is maximum. This behavior is illustrated in Fig. 3, where the group index and transmission at the first slow-light peak for a uniform grating with $\Delta n = 1.0 \times 10^{-3}$. Loss clearly induces a sharp reduction in the group index. However, a real grating can still support remarkably low velocities because its loss is inherently so low. For example, for the lowest loss coefficient (0.4 m^{-1}) the predicted maximum n_g is equal to 154.4. It occurs for a length of only 3.1 cm, and the transmission is then 10.73%. The same grating of same length without loss would support an n_g of 465.6 for a $\sim 100\%$ transmission.

Light can be slowed down even further with suitable apodization to provide the proper phase matching between the input light and the grating. Consider as an example the apodized profile in the inset of Fig. 4, which has a Gaussian envelope with a full width at half maximum W. Fig. 4(a) plots the transmission spectrum and Fig. 4(b) the group index spectrum of this type of grating with $L = 1.2$ cm, $\Delta n = 1.0 \times 10^{-3}$, $W = 0.98$ cm, and $\alpha = 1\ \mathrm{m}^{-1}$. The transmission spectrum is asymmetric with respect to λ_B [see Fig. 4(a)]. The side-lobes on the long-wavelength side are greatly reduced, while the side-lobes on the short-wavelength side support much lower group velocities [see Fig. 4(b)] than a uniform grating of same length and peak index modulation.

When $W \ll L$, the effective length of the grating decreases and the group index drops. When $W \gg L$, the FBG behaves asymptotically like a uniform grating. Between these two extremes there is an optimum width W that minimizes the group index. As an example, the optimized length for an H_2-loaded grating with $\Delta n = 4.5 \times 10^{-3}$, $\alpha = 3.7\ \mathrm{m}^{-1}$, and $W = 2L$ is 3.3 mm [15]. At this length, the group index is as high as ~ 212, which is much larger than if the apodization was removed and everything else kept the same (which would give an n_g of only 70.2).

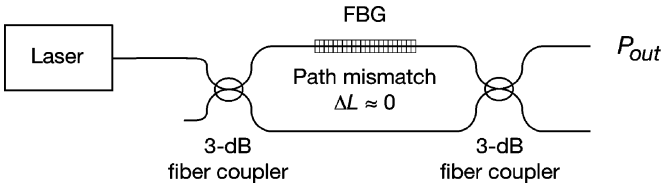

Fig. 5. Diagram of slow-light FBG sensor operated in transmission using a nominally balanced Mach–Zehnder interferometer.

B. Modeling the Sensitivity of a Slow-Light FBG Sensor

A general approach to generating a slow-light FBG sensor is to place the FBG in the arm of an interferometer and probe this interferometer at a slow-light wavelength. The role of the interferometer is to convert the enhanced phase modulation resulting from a perturbation applied to the FBG into an enhanced amplitude modulation, which is measured directly at the interferometer output. One of several possible implementations of this principle is to use an MZI, as illustrated in Fig. 5. Light from a narrowband laser at a wavelength in the vicinity of one of the FBG's slow-light peaks is launched into the MZI. Because the phase modulation is generated inside the interferometer, the latter does not need to be imbalanced. Using a nominally balanced MZI has two benefits. First, the laser phase noise is not converted into amplitude noise by the MZI, and the noise in the detected signal is reduced. Second, the MZI can be very short and therefore comparatively stable against external perturbations such as temperature changes.

Because the transmission at a slow-light wavelength is less, and often significantly less, than 100%, it is necessary to take it into account when calculating the sensitivity of the sensor of Fig. 5. The MZI output field is the coherent sum of the field transmitted by the upper (sensing) arm, which contains the FBG, and the field transmitted by the lower (or reference) arm. It is easy to show that the MZI output power resulting from this coherent sum is given by

$$P_{\text{out}} = P_0 \left((1-\eta)^2 T_1 + \eta^2 T_2 - 2\eta(1-\eta)\sqrt{T_1 T_2}\cos(\Delta\phi) \right) \tag{2}$$

where P_0 is the power incident on the leftmost coupler, η is the coupler's coupling coefficient, $\Delta\phi$ is the propagation phase difference between the two arms, and T_1 and T_2 are the power transmission of the upper and lower arm, respectively. $\Delta\phi$ is the sum of a constant term, which is the built-in phase difference (or phase bias) between the two arms, and the phase perturbation $\delta\phi$ applied to the FBG. The MZI sensitivity to a small $\delta\phi$ is maximum when the phase bias is $\pi/2$ (modulo π). For a dynamic perturbation, the term that is detected at the output of the sensor is the third term in (2). Thus (2) becomes

$$P_{\text{out}}(\delta\phi) \approx 2P_0\eta(1-\eta)\sqrt{T_1 T_2}\delta\phi. \tag{3}$$

The strain sensitivity is by definition

$$S = \frac{1}{P_0}\frac{dP_{\text{out}}}{d\varepsilon} = \frac{1}{P_0}\frac{dP_{\text{out}}}{d\phi}\frac{d\phi}{d\lambda}\frac{d\lambda}{d\varepsilon}. \tag{4}$$

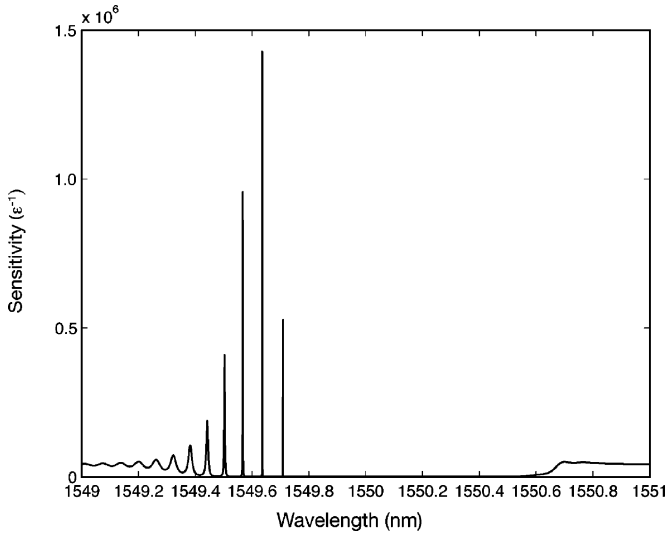

Fig. 6. Calculated sensitivity spectrum of the FBG of Fig. 4.

The derivative $dP_{\text{out}}/d\phi$ is obtained simply from (3). The rate of change of the optical phase with wavelength $d\phi/d\lambda$ is given in general terms by [1]

$$\frac{d\phi}{d\lambda} = n_g \frac{L}{c}\frac{d\omega}{d\lambda}. \tag{5}$$

Finally, the last derivative in (4) relates the rate of wavelength shift of the FBG's reflection spectrum to a small applied strain $d\varepsilon$. This shift arises from three effects, as mentioned earlier. When ignoring the smaller third effect (the change in mode effective index due to the strain-induced change in the fiber core size), this term is equal to [16]

$$\frac{d\lambda}{d\varepsilon} = -\lambda_B \left[1 - \frac{n^2}{2}\left(p_{12} - \nu(p_{11}+p_{12}) \right) \right] \tag{6}$$

where p_{11} and p_{12} are the elasto-optic coefficients of the fiber, ν is Poisson's ratio, and n is the mode effective index. For a silica fiber, $d\lambda/d\varepsilon = -0.79\lambda_B$. Combining these three derivatives (4) yields the strain sensitivity

$$S = 3.16\pi\eta(1-\eta)\sqrt{T_1 T_2}\, n_g L \frac{\lambda_B}{\lambda^2}. \tag{7}$$

Equation (7) states that the output power is proportional to $\eta(1-\eta)(T_1T_2)^{1/2}n_g$. The sensitivity is maximum when $\eta = 0.5$ (50% coupling at both MZI couplers), as expected, but also when T_1 and T_2 are maximum. It is straightforward to make the reference arm essentially lossless, so we will assume $T_2 = 1$. The bottom line is that to maximize the sensitivity one must maximize not n_g alone, but the product $n_g\sqrt{T_1}$, the relevant figure of merit that maximizes the sensitivity.

Since the relevant figure of merit is $n_g\sqrt{T_1}$, it is not necessarily the first slow-light peak (closest to the band edge) that produces the highest sensitivity, because its transmission is too weak. For example, consider the example of the FBG of Fig. 4. Its sensitivity is proportional to the product of the n_g spectrum [Fig. 4(b)] and the square root of the transmission spectrum [Fig. 4(a)]. This product is shown in Fig. 6. It is clear from this figure that for this particular FBG, the sensitivity is maximum not at the first but at the second slow-light peak. This derivation

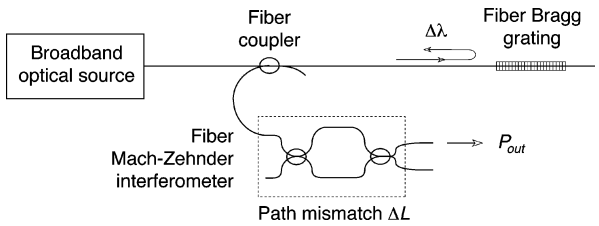

Fig. 7. Conventional strain-sensing scheme using an FBG in reflection.

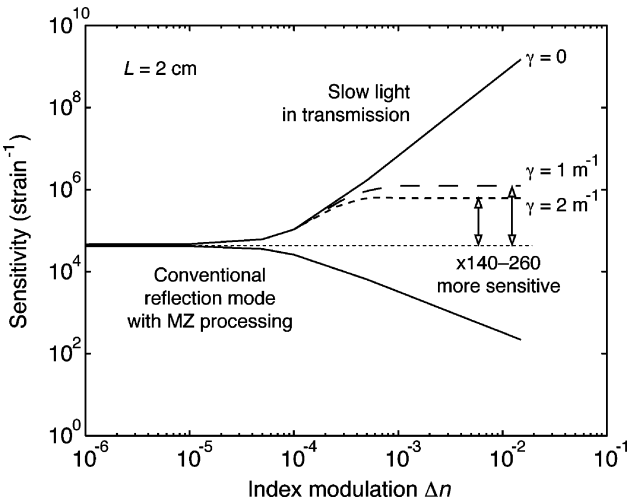

Fig. 8. Calculated strain sensitivity dependence on index modulation for the proposed slow-light FBG sensor and the conventional FBG reflection sensor using an imbalance MZI for signal processing.

provides a quick method to compute the sensitivity spectrum of a given FBG, and to assess the wavelength of maximum sensitivity, as well as the maximum sensitivity.

Long ago scientists at NRL demonstrated a clever signal-processing scheme to enhance the sensitivity of FBG sensors operated in reflection (Fig. 7) [17]. The reflected signal returning from the FBG, which is shifted from its original wavelength by a quantity $\Delta\lambda$ proportional to the perturbation applied to the FBG (e.g., a strain), is sent through a path-imbalanced MZI. The latter converts the wavelength shift into a shift in intensity proportional to $\Delta\lambda$ and to the MZI path mismatch ΔL. The sensitivity of this scheme can therefore be increased by increasing the path mismatch, but only up to a point. First, as the path mismatch is increased the MZI's thermal stability worsens. Second, and more fundamentally, for interference to occur at the MZI's output the path mismatch must not exceed the coherence length of the signal in the fiber. This coherence length is ultimately limited by the index modulation Δn of the grating: the lower Δn the longer the coherence length, which means that to increase the sensitivity one must use a very weak, and therefore very long, grating (in order to achieve sufficient reflectivity), which is more difficult to make and less thermally stable. This scheme encourages the use of weaker FBGs, which do not support slow light. It has nevertheless produced the lowest MDS reported in a passive FBG that does not rely on slow light. As such, it is a worthy metric against which to compare our slow-light scheme.

Fig. 8 plots the strain sensitivity of our slow-light FBG sensor as a function of index modulation, and compares it to the sensitivity of the scheme of Fig. 7. Both FBGs have a length of 2 cm. The FBG in the conventional scheme is assumed lossless, for simplicity. For the conventional sensor, the sensitivity is maximum when the grating is very weak, and it drops as the index modulation increases, as explained in the preceding paragraph. In contrast, the sensitivity of the slow-light sensor increases steadily (and quickly for larger Δn) as Δn is increased. In the lossless limit, it can be as much as five orders of magnitude more sensitive. In practice, for a loss of 1 m^{-1} it is predicted to be $\sim$ 260 times more sensitive. This improvement is achieved again concomitantly with the use of a more stable signal processing scheme (a balanced MZI). This figure illustrates the tremendous potential for increased sensitivity afforded by the use of slow light.

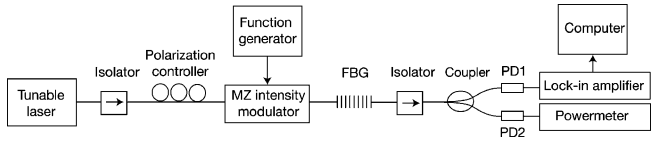

Fig. 9. Diagram of the group delay measurement setup.

III. Experimental Studies

Several commercial FBGs with different index modulations, modulation profiles, and lengths were evaluated to confirm the various predictions of the above theoretical section. The first goal was to achieve group indices as high as possible, i.e., to acquire FBGs with index modulations as high as possible and losses as low as possible. The second goal was to measure the sensitivity of slow-light FBGs to dynamic strains and confirm that this new kind of sensor is more sensitive than existing passive FBG strain sensors that do not rely on slow light.

A. Measurements of Slow-Light Velocity

To evaluate the slow-light properties of strong FBGs, we measured the transmission and group index spectra of FBGs using the experimental setup of Fig. 9. Light from a tunable laser with a narrow linewidth (100 kHz) and fine wavelength resolution (0.1 pm) was modulated sinusoidally at $f_m = 25$ MHz using an external intensity modulator. The modulated light was coupled into the FBG under test. The signal exiting the FBG was split using a 50/50 fiber coupler. One output signal was sent to a power meter to measure (by varying the laser wavelength) the power transmission spectrum of the FBG. The other output was sent to a photodetector followed by a lock-in amplifier, which measured its phase. The first measurement was conducted at 1548 nm, i.e., far enough from the band edge (2 nm) that the group velocity is normal. The measured phase at this wavelength was thus used as a reference value that corresponded to a known group index equal to the index of silica $n_0 \approx 1.44$. The wavelength was then tuned close to the band edge and the phase measurement was repeated. The difference in group delay between the two wavelengths was calculated from the phase change $\Delta\phi$ measured between these two wavelengths using

$$\Delta\tau_g = \frac{\Delta\phi}{2\pi f_m}. \tag{8}$$

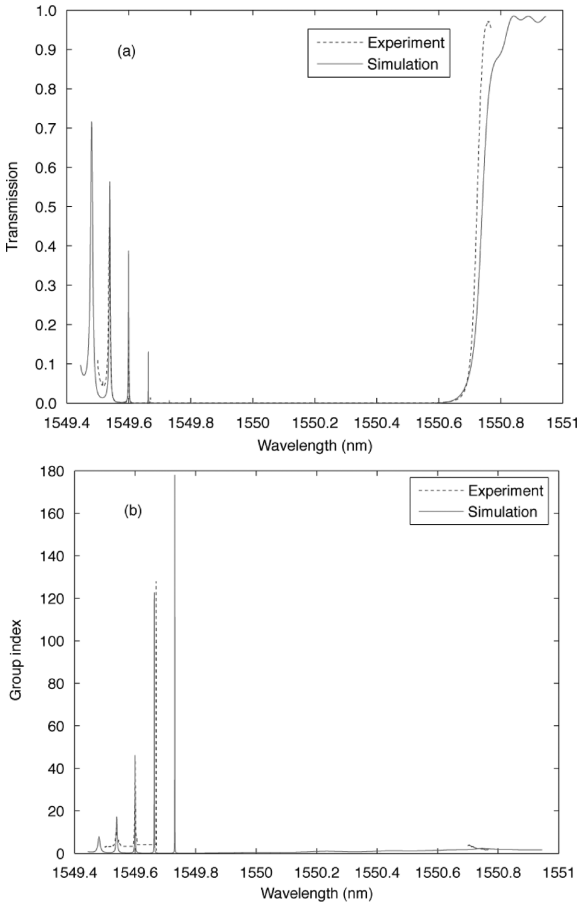

Fig. 10. Measured spectrum of the signal transmitted by a strong FBG: (a) transmission and (b) group index.

The group index at the second wavelength was then calculated from $\Delta\tau_g$ using

$$n_g = \Delta\tau_g \frac{c}{L} + n_0. \tag{9}$$

Fig. 10(a) shows the measured transmission spectrum and Fig. 10(b) the group index spectrum of the signal transmitted by the FBG that yielded the lowest group velocity we have been able to observe so far. Both measured spectra exhibit multiple slow-light peaks on the short-wavelength side of the bandgap, and virtually no peaks on the long-wavelength side, as expected theoretically for an apodized FBG (see Fig. 4). We were able to observe five peaks. The maximum measured group index occurs in the vicinity of the second transmission peak ($\lambda \approx 1549.6976$ nm) and is equal to 127. The transmission at this wavelength is 0.8%. This is the slowest group velocity ($\sim 2{,}360$ km/s) reported in an FBG. The peak closest to the band edge ($\lambda \approx 1.54974$ μm) should have an even higher group index (~ 217), but it could not be measured because the transmitted power at this peak was too small to detect, even with optical amplification of the signal incident on the MZI. The corresponding solid curves in Fig. 10 are theoretical predictions calculated with our model after adjusting Δn, W, and α to best fit them to the experimental spectra. The fitted values are $\Delta n = 1.035 \times 10^{-3}$, $L = 1.2$ cm, $W = 0.9$ cm, and $\alpha = 1.16$ m^{-1}. The former two values agree well with the manufacturer's estimated values (10^{-3} and 1.2 cm). Both measured spectra agree well with theory. This breakthrough result confirms that much slower light can be achieved in a device as simple as an FBG as was believed before. Even larger group indices can be achieved in lower loss FBGs.

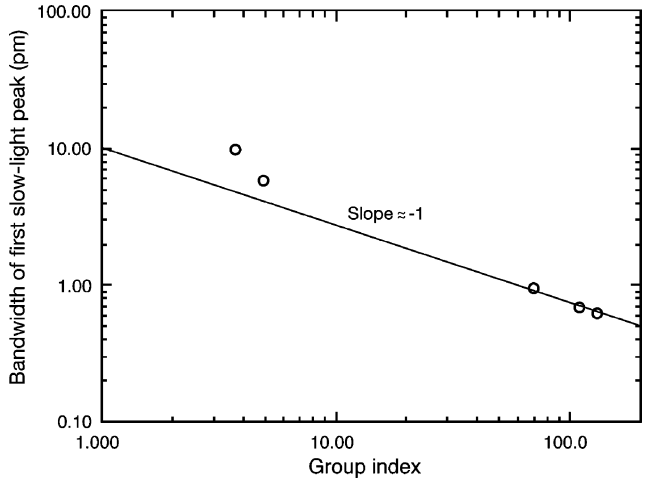

Fig. 11. The experimentally measured bandwidth and group index for various FBGs.

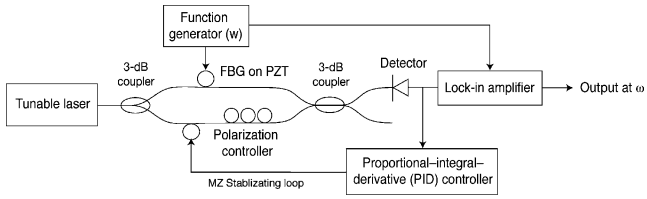

Fig. 12. Diagram of the slow-light FBG strain sensor.

In our study, five FBGs with various lengths, index modulations, index profiles, and loss coefficients were characterized. Fig. 11 shows the relationship between the measured 3-dB bandwidth of the first slow-light peak and the group index for these FBGs. The bandwidths range from 11 pm in a weak FBG with $n_g \approx 3.7$ to 0.62 pm in a strong FBG with $n_g \approx 127$. Although these FBGs have different parameters, the slope fitted to these data points is about -1.0 pm, i.e., the bandwidth is inversely proportional to the group index. The group delay in the FBG that produced the slowest light is ~ 5 ns, and the delay-bandwidth product is 0.39. This is lower than products achieved with SBS ($\sim$ 30-ns delay with a 40 MHz bandwidth [4], or a product of ~ 1.2). As shown in Section II, FBGs can support much larger group indices, and thus delays, comparable to what is achievable with SBS.

B. Measurements of Strain Sensitivity

The strain sensitivity of this FBG was measured by placing it in an MZI according to the configuration of Fig. 5. A diagram of the experimental sensor is shown in Fig. 12. To apply a controlled and calibrated strain to the FBG, it was mounted on a piezoelectric (PZT) ring, and an AC voltage was applied to the

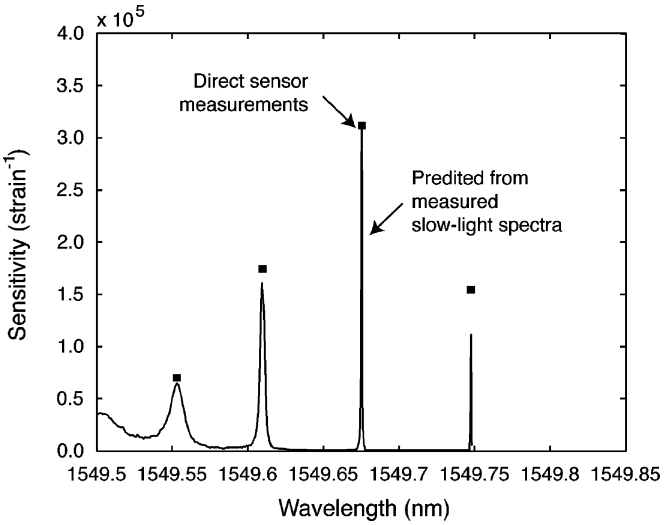

Fig. 13. Measured strain sensitivity of the FBG sensor and theoretical sensitivity spectrum predicted from its measured group index and transmission spectra.

ring at a frequency $f = 25$ kHz. The FBG was then placed in the fiber MZI, which was made with two 3-dB fiber couplers, short lengths of fiber, and optical connectors. Care was taken to make sure that the two arms of the MZ interferometer had the same length within 1–3 mm to minimize conversion of laser phase noise into intensity noise. The MZI output was measured with a low-noise photodetector. This output contains a slowly varying component due to slow thermally induced variations in the phase difference between the two arms of the MZI. This variable signal was sent to a proportional-integral-derivative (PID) controller, which provided feedback to a second PZT ring placed in the reference arm to cancel out this slow drift. The purpose of this closed loop was first to stabilize the interferometer against the aforementioned thermally induced phase variations, and second to maintain its phase bias at $\pi/2$ for maximum sensitivity. Another portion of the detector output was sent to a lock-in amplifier, which extracted from it the f component of the output. The sensitivity of the sensor was measured by varying the wavelength of the tunable laser, and measuring for each wavelength the response to the same known applied strain. The PZT on which the FBG was attached was calibrated beforehand by wrapping a known length of fiber around it, placing the fiber inside a separate MZI, and measuring the phase shift in this fiber, from which the strain could be calculated, as a function of the PZT voltage.

The result of the strain-sensing experiment is plotted in Fig. 13 in the form of the sensitivity measured at four of the observed slow-light peaks. The maximum measured value occurs at the second slow-light peak. It is equal to $S = 3.14 \times 10^5\ \mathrm{strain}^{-1}$. The theoretical sensitivity spectrum of this sensor is also shown in Fig. 13. It was calculated from this FBG's measured group index and transmission spectra (Fig. 10) and the $n_g(\lambda)\sqrt{T_1(\lambda)}$ dependence in (7). Importantly, no fit was performed to obtain this sensitivity spectrum. There is excellent between the measured and the predicted sensitivity spectrum in Fig. 13, which confirms a sound understanding of the mechanism that is taking place in this sensor, and the key role of slow light in its ultrahigh sensitivity.

To compare the sensitivity performance of this sensor to that of other strain sensors of its class, namely passive FBG-based strain sensors, we calculated its MDS, the metric most often used in the literature. At the mean detected power in our measurements ($P_d = 20\ \mu$W for a power input into the MZI of $P_0 = 36\ \mu$W), the measured noise at the output of the unstrained sensor was $P_{noise} = 10\ \mathrm{pW}/\sqrt{\mathrm{Hz}}$. This noise was composed approximately equally of laser relative intensity noise (RIN) and photodetector noise. Laser phase noise was negligible because the MZI was very nearly balanced. From the definition of the sensitivity, the MDS (the strain that produces a variation in output power equal to the noise) can be written as

$$\varepsilon_{min} = \frac{1}{S}\frac{P_{noise}}{P_0}. \tag{10}$$

At the highest measured sensitivity ($3.14 \times 10^5\ \mathrm{strain}^{-1}$), the MDS of our sensor is 880 $\mathrm{f}\varepsilon/\sqrt{\mathrm{Hz}}$. The measured sensitivity is ~ 700 times lower than the lowest value reported to date using the conventional passive scheme of Fig. 7 (600 $\mathrm{p}\varepsilon/\sqrt{\mathrm{Hz}}$), which did not rely on slow light. [17] A detailed comparison between these two sensors would be needed to produce a calibrated comparison, yet it is meaningful that the improvement brought about by the use of slow light is of the order of magnitude predicted in Fig. 8 (a factor of ~ 260). We reiterate that [17] achieved its sensitivity without using slow light, and also that it utilizes an MZI configuration, therefore it is quite relevant for our comparison purposes. On the other hand, it is interesting to note that two other published approaches have led to an even better MDS than the conventional result of [17]. One is an FBG that was probed in reflection not at λ_B as is customary but at a wavelength on the falling edge of the bandgap [18]. This scheme achieved an MDS of 45 $\mathrm{p}\varepsilon/\sqrt{\mathrm{Hz}}$. Our model shows, as expected on physical grounds, that in the vicinity of this wavelength the group velocity of light is also reduced, although not as much as at the wavelengths reported in this paper. Although the concept of slow light was not mentioned in [18], it is our opinion that this reference did utilize slow light, and that the low MDS they report is likely due mostly to slow light. Also, in [19], strain detection was effected by probing a π-shifted FBG in the vicinity of the narrow high-transmission peak that exists in the middle of its bandgap. An MDS of 5 $\mathrm{p}\varepsilon/\sqrt{\mathrm{Hz}}$ was demonstrated. Again, although no mention of slow light is made in [19], we believe that this very low detectable strain was made possible by the use of the low group velocity that prevails in a π-shifted grating in the vicinity of the narrow central transmission.

In the light of this prior art, we conclude that with an MDS of 880 $\mathrm{f}\varepsilon/\sqrt{\mathrm{Hz}}$ our sensor is the most sensitive passive FBG strain sensor reported to date. This is a factor of ~ 6 more sensitive than the next best value for a passive FBG strain sensor that we believe utilized slow light [19], and 700 times more sensitive than the next best FBG sensor that did not rely on slow light [17].

As expected, this increased sensitivity arising from the use of slow light comes at the price of a reduced bandwidth because slow light exists over a limited range of frequencies, and this range generally decreases as the group delay increases. However, the bandwidth still remains sizeable. For example, in the strain sensor of Fig. 13, the measured bandwidth for 90% of the highest detectable elongation is 0.2 pm, which corresponds to a

maximum strain of 0.16 $\mu\varepsilon$. The dynamic range is $\sim 180\,000$, which is comparable to that of typical interferometric fiber sensors ($\sim 10^5 - 10^6$).

IV. Conclusion

In conclusion, we have shown theoretically for the first time that an FBG with a large index modulation and an optimized length and apodization can support light with a much lower group velocity than previously anticipated. We have verified this principle by demonstrating a group velocity of 2360 km/s (a group index of 127) in a 1.2-cm apodized FBG with a Δn of 1.035×10^{-3} and a loss of $\sim 1\ \mathrm{m}^{-1}$. This is the slowest light reported to date in an FBG. Using the strongest detectable slow-light peak in this FBG, we demonstrated a strain sensor with a sensitivity of $3.14 \times 10^5\ \mathrm{strain}^{-1}$ and a minimum detectable strain of 880 $\mathrm{f}\varepsilon/\sqrt{\mathrm{Hz}}$, the world record for a passive FBG strain sensor. This is the first demonstration that slow light can significantly enhance the sensitivity to a perturbation in an optical fiber grating. These results point to a novel class of fiber devices and sensors with unprecedented properties and valuable potential applications in many branches of photonics.

References

[1] M. Soljačić, S. G. Johnson, S. Fan, M. Ibanescu, E. Ippen, and J. D. Joannopoulos, "Photonic-crystal slow-light enhancement of nonlinear phase sensitivity," *JOSA B*, vol. 19, no. 9, pp. 2052–2059, 2002.

[2] M. Digonnet, "New technologies in fiber sensors," in *Proc. CLEO Europe 2007*, Munich, Germany, 2007, CH2-1.

[3] A. D. Slepkov, A. R. Bhagwat, V. Venkataraman, P. Londero, and A. L. Gaeta, "Generation of large alkali vapor densities inside bare hollow-core photonic band-gap fibers," *Opt. Express*, vol. 16, no. 23, pp. 18976–18983, 2008.

[4] K. Y. Song, M. Gonzalez-Herraez, and L. Thévenaz, "Optically controlled slow and fast light in optical fibers using stimulated Brillouin scattering," *Appl. Phys. Lett.*, vol. 87, no. 8, p. 081113, 2005.

[5] J. T. Mok *et al.*, "Dispersionless slow light using gap solitons," *Nature Phys.*, vol. 21, pp. 775–780, 2006.

[6] C. J. Misas, P. Petropoulos, and D. J. Richardson, "Slowing of pulses to $\mathrm{c}/10$ with subwatt power levels and low latency using Brillouin amplification in a bismuth-oxide optical fiber," *J. Lightw. Technol.*, vol. 25, no. 1, pp. 216–221, 2007.

[7] M. Lee *et al.*, "Improved slow-light delay performance of a broadband stimulated Brillouin scattering system using fiber Bragg gratings," *App. Opt.*, vol. 47, no. 34, pp. 6404–6415, 2008.

[8] J. T. Mok, C. M. de Sterke, and B. J. Eggleton, "Delay-tunable gap-soliton-based slow-light system," *Opt. Express*, vol. 14, pp. 11987–11996, 2006.

[9] T. Erdogan, "Fiber grating spectra," *J. Lightw. Techno.*, vol. 15, no. 8, pp. 1277–1294, 1997.

[10] A. Yariv, *Optical Waves in Crystals: Propagation and Control of Laser Radiation*. New Work: Wiley, 1984, p. 197.

[11] P. J. Lemaire, R. M. Atkins, V. Mizrahi, and W. A. Reed, "High pressure H_2 loading as a technique for achieving ultrahigh UV photosensitivity and thermal sensitivity in GeO_2 doped optical fibers," *Electron. Lett.*, vol. 29, no. 13, pp. 1191–1193, 1993.

[12] Y. Liu, L. Wei, and J. W. Y. Lit, "Transmission loss of phase-shifted fiber Bragg gratings in lossy materials: A theoretical and experimental investigation," *App. Opt.*, vol. 46, no. 27, pp. 6770–6773, 2007.

[13] D. Johlen, F. Knappe, H. Renner, and E. Brinkmeyer, "UV-induced absorption, scattering and transition losses in UV side-written fibers," in *Proc. Conf. Opt. Fiber Commun., OFC'99*, 1999, THD1.

[14] M. Bernier, Private Communication. Québec, Canada, Université Laval.

[15] M. Bernier, Y. Sheng, and R. Vallée, "Ultrabroadband fiber Bragg gratings written with a highly chirped phase mask and Infrared femtosecond pulses," *Opt. Express*, vol. 17, no. 5, pp. 3285–3290, 2009.

[16] A. D. Kersey, M. A. Davis, H. J. Patrick, M. LeBlanc, K. P. Koo, C. G. Askins, M. A. Putnam, and E. J. Friebele, "Fiber grating sensors," *J. Lightw. Technol.*, vol. 15, no. 8, pp. 1442–1463, 1997.

[17] A. D. Kersey, T. A. Berkoff, and W. W. Morey, "High resolution fibre-grating based strain sensor with interferometric wavelength-shift detection," *Electron. Lett.*, vol. 28, no. 3, pp. 136–138, 1992.

[18] B. Lissak, A. Arie, and M. Tur, "Highly sensitive dynamic strain measurements by locking lasers to fiber Bragg gratings," *Opt. Lett.*, vol. 23, no. 24, pp. 1930–1932, 1998.

[19] D. Gatti, G. Galzerano, D. Janner, S. Longhi, and P. Laporta, "Fiber strain sensor based on a π-phase-shifted Bragg grating and the Pound-Drever-Hall technique," *Opt. Express*, vol. 16, no. 3, pp. 1945–1950, 2008.

He Wen received the B.A.Sc. degree in electrical engineering from the University of British Columbia, Vancouver, Canada, in 2006, and the M.S. degree in electrical engineering from Stanford University, Stanford, CA, in 2008.

Matt Terrel received the B.S. degree in physics from the California Institute of Technology, Pasadena, CA, in 2004, and the M.S. degree in applied physics from Stanford University, Stanford, CA, in 2006.

His research interests include various aspects of optical fiber sensors.

Shanhui Fan (SM'06–F'11) was an undergraduate student in physics at the University of Science and Technology of China, Hefei, Anhui, China, from 1988 to 1992, and received the Ph.D. degree in physics from the Massachusetts Institute of Technology (MIT), Cambridge, in 1997.

He is an Associate Professor of Electrical Engineering at Stanford University, Stanford, CA. He was a Postdoctoral Research Associate in Physics at MIT from 1997 to 1999 and a Research Scientist at the Research Laboratory of Electronics, MIT, from 1999 to 2001. He has been at Stanford University since 2001. He has published over 220 journal articles, has given more than 150 invited talks, and held 39 granted U.S. patents. His interests include theory and simulations of photonic and solid-state materials and devices, photonic crystals, nanoscale photonic devices and plasmonics, quantum optics, computational electromagnetics, and parallel scientific computing.

Michel Digonnet (M'01) received the Engineering degree from Ecole Supérieure de Physique et de Chimie de la Ville de Paris, Paris, France, the Diplome d'Etudes Approfondies in coherent optics from the University of Paris, Orsay, France, in 1978, and the M.S. and Ph.D. degrees from the Department of Applied Physics, Stanford University, Stanford, CA, in 1980 and 1983, respectively. His doctoral research centered on WDM fiber couplers and single-crystal fiber lasers and amplifiers.

He is currently a Research Professor in the Department of Applied Physics, Stanford University. From 1983 to 1986, he was employed by Litton Guidance and Control, Chatsworth, CA, conducting research in miniature solid-state sources and integrated optics for fiber-optic gyroscopes. From 1986 to 1990, he was involved in the development of delivery systems for laser angioplasty at MCM Laboratories, Mountain View, CA. He has published about 250 articles, issued 90 U.S. patents, edited several scientific books, taught courses in fiber amplifiers, lasers, and sensors, and chaired numerous conferences on various aspects of photonics. His current interests include fiber sensors, photonic-bandgap fibers and devices, slow and fast light in sensors, and fiber-based MEMS hydrophones and microphones.